SUBCORTICAL MULTISENSORY LOOP IN THE ASCENDING TECTOFUGAL SYSTEM

Doctoral thesis

Dr. Zita Márkus

Supervisors: Prof. Dr. György Benedek
Dr. Attila Nagy

Department of Physiology
Faculty of Medicine, University of Szeged

Szeged, 2009

Table of contents

1. List of publications providing the basis of the thesis

I. Multisensory integration in the basal ganglia

Nagy A, Eördegh G, Paróczy Z, **Márkus Z**, Benedek G.

Eur J Neurosci 24:917–924. (2006)

IF: 3.385

II. Spatial and temporal visual properties of single neurons in the suprageniculate nucleus of the thalamus

Paróczy Z, Nagy A, **Márkus Z**, Waleszczyk WJ, Wypych M, Benedek G.

Neuroscience 137:1397–1404. (2006)

IF: 3.556

III. Modality distribution of sensory neurons in the caudate nucleus and the substantia nigra

Márkus Z, Eördegh G, Paróczy Z, Benedek G, Nagy A

Acta Biol Hung 59:269–279. (2008)

IF: 0.619

IV. Drifting grating stimulation reveals particular activation properties of visual neurons in the caudate nucleus

Nagy A, Paróczy Z, **Márkus Z**, Berényi A, Wypych M, Waleszczyk WJ, Benedek G.

Eur J Neurosci 27:1801–1808. (2008)

IF: 3.385

V. Spatial and temporal visual properties of the neurons in the intermediate layers of the superior colliculus

Márkus Z, Berényi A, Paróczy Z, Wypych M, Waleszczyk WJ, Benedek G, Nagy A.

Neurosci Lett 454:76–80. (2009)

IF: 2.200

2. Introduction

2.1. General principles concerning multisensory information processing and integration

Encoding, decoding and interpreting information about biologically significant events are the brain's most important functions and they require a huge neural circuitry. These functions have been important driving forces in evolution and have led to the development of the specialized sensory organs, each of which is connected to more specialized brain regions.

Researchers and science philosophers have been impressed for more thousands of years by how the individual senses are capable of working together and enhance biologically meaningful events. However, they had no idea how this was accomplished.

The advantages of having multiple senses include the usefulness of each senses under different circumstances, thus, the different senses together are able to increase the likelihood of detecting and identifying objects or events of interest. Even more advantage arises from the fact that different brain structures are capable of combining sources of information. In this case the integrated product reveals more data about the external event and does so better and faster than would be predicted from the sum of its individual components. This synergy or interaction among the function of the senses is described by the term "multisensory integration".

Multisensory integration can be evaluated by considering the effectiveness of a cross-modal stimulus combination, related to that of its component stimuli, for eliciting some kind of response from the neuron or the organism. For example, the probability of a response to an event or an object that has both visual and somatosensory components is compared with that for the visual and somatosensory stimulus alone. At the level of the single neuron multisensory integration is defined as the statistically significant difference between the number of impulses evoked by a cross-modal stimulus combination and the number evoked by the most effective of these stimuli individually [1].

Thus, multisensory integration can result in either enhancement or depression of the neuronal response. Sensory stimuli compete for the attention, therefore the consequence of multisensory enhancement or depression is an increased or decreased possibility of detecting and initiating a response to the source of the information. The magnitude of multisensory integration can vary widely according to different types of neurons and even

for the same neuron when stimulated with different cross-modal stimulus combinations. The largest multisensory enhancements are due to superadditive combinations of cross-modal stimulus combinations and the smallest ones are due to subadditive combinations (cross modal inhibitions). Multisensory integration can also shorten the response onset latency time between encoding of the sensory information and forming of the motor command and it can also speed the sensory processing itself [1].

The advantages and benefits of multisensory integration for orienting behavior have received a huge amount of attention and provided a lot of information about the underlying neural mechanisms of multisensory integration in different structures of the brain, especially the midbrain and the cerebral cortex of cats and monkeys. However, we know much less about the physiological processes underlying higher-order multisensory functions, such as perceptual binding.

2.2. Multisensory information processing and integration in the midbrain of the cat and the monkey

The most important midbrain structure involved in multisensory information processing and integration in the brain of cats and monkeys is the superior colliculus (SC). The SC is a multilayered structure of the mammalian midbrain, which plays an important role in visually guided behavior and is involved in the orienting response of the head and the eyes toward the object of interest of any modality [2-4]. The superficial layers of the SC (SCs) receive direct retinal input [5;6] and also afferentation from the primary visual cortex [7-9]. They project upon the dorsal lateral geniculate nucleus (LGNd), the lateral posterior pulvinar complex (LP-Pul) and the pretectum [10;11]. The intermediate and deep layers (SCi) receive input from the association cortical areas, i.e. the anterior ectosylvian cortex (AES cortex) and the posteromedial lateral suprasylvian area (PMLS), from the somatosensory and auditory cortex [7], and from the substantia nigra (SN), the pedunculopontine tegmental nucleus and the cerebellum [11]. The superficial layers project to the medial LP-Pul of the visual thalamus, while the intermediate and deep layers also send axons to the suprageniculate nucleus (Sg) of the posterior thalamus. [11-13]. As concerning the physiological differences, the SCs layers (the stratum griseum superficiale and stratum opticum) have exclusively visual properties, while the deeper layers (the layers under the stratum opticum) are multisensory, processing auditory and somatosensory

information as well [14]. The layers of the SCs seem to play a role in the central processing of visual information, e.g. visual attention, motion perception and orientation behavior [15;16]. The SCi layers are regarded as important structures for the control of saccadic eye movements [3] and in cross-modal integration [14]. Descending excitatory inputs from the AES and lateral suprasylvian (LS) cortices are essential for multisensory integration in the SCi neurons. Besides being a crucial part of the oculomotor system, the SCi layers are involved in the control of head movements [17;18] and goal-directed arm movements [19;20].

2.3. Multisensory information processing and integration in the cerebral cortex of the cat and the monkey

In the feline cerebral cortex the association cortical areas along the anterior ectosylvian sulcus (AES) and the lateral suprasylvian sulcus (LS) have been described as multisensory areas, where inputs from several sensory modalities converge [21]. The AES is situated at the junction between the frontal, the parietal and the temporal cortices. It is composed of distinct somatosensory (SIV, the fourth somatosensory area [22]), visual (AEV, the anterior ectosylvian visual area [23;24]) and auditory (FAES, the auditory field of the AES [25]) regions. Near the borders of these unimodal regions those neurons are located which respond to more than one sensory modality stimulus. The LS is an area of the parietal cortex important in visual information processing [26].

Multisensory neurons in the feline SCi receive descending projections from the AES and LS cortices [21;27-33]. These projections are essential for the multisensory information processing and integration ability of the neurons in the SCi. In the absence of these descending cortical inputs to the SCi, some SCi neurons can remain multisensory, due to their other inputs. However, the ability to integrate these inputs is lost when the descending cortical projections are missing, i.e. the neurons lose their multisensory integration ability [29;30].

In addition to the cerebral cortex of the cat, neurophysiological and functional-imaging studies have identified many multisensory cortical regions in non-human primates. These regions include in monkeys the lateral intraparietal area (LIP, visually and auditory sensitive neurons [34]), the parietal reach region in the medial intraparietal area (MIP, visually, auditory and somatosensory sensitive neurons [35;36]), the ventral

intraparietal area (VIP, visually, auditory, somatosensory and vestibular sensitive neurons [37]), which are all parts of the posterior parietal cortex (PPC). The ventrolateral prefrontal cortex (VLPFC, auditovisual congruence, vocalization [38;39]) and the superior temporal sulcus (STS, vocalization, auditovisual congruence [40]) have also been identified as multisensory cortical areas.

2.4. Multisensory information processing and integration in the human brain

Most studies of multisensory information processing and integration in the human cortex have been carried out by neuroimaging and evoked-potential examinations [41]. Local field potential (LFP) studies have revealed multisensory integration in some regions of the auditory cortex [42].

Earlier human neuroimaging studies suggested that the STS is specifically responsible for integrating auditory and visual speech signals [43]. During these studies, the blood-oxygen-level-dependent (BOLD) signal increased for congruent pairings of audible speech and lip movements and decreased for incongruent pairings [43].

Functional imaging studies have described several multisensory regions in the human cortex. Trisensory (visually, auditory and somatosensory sensitive) neurons have been found in the superior prefrontal cortex, the premotor cortex and also the parietal cortex. Visually and auditory sensitive neurons are located in the cortical areas along the posterior part of the STS. Visually and somatosensory sensitive neurons have been revealed in the inferior prefrontal cortex and also in the parietal cortex [44].

The observations that many areas that were previously classified as unisensory contain multisensory neurons are also supported by anatomical studies showing connections between unisensory cortices [45-49].

2.5. Sensory information processing in the ascending tectofugal system

The ascending tectofugal sensory-motor system of the feline brain has been in the focus of attention of our research group for the past few decades. This system derives from the SCi and projects to the Sg nucleus of the extrageniculate thalamus. From this central nucleus fibers reach both association cortical areas, such as the AEV and also the basal ganglia, especially the caudate nucleus (CN) and the SN. This thesis summarizes our research results obtained from the SCi and the basal ganglia.

Despite numerous studies focusing on the visual receptive field organization and properties of the SC neurons ([50-52]; for earlier literature, see [53-55]), very little information is available concerning the responsiveness of the SCi neurons to extended visual stimuli, such as sinewave drifting gratings. The sinusoidally modulated gratings are regarded as elementary components of the visual scene in the sense that any two-dimensional visual object can be represented by an appropriate combination of these gratings [56;57]. None of the published studies has yielded a detailed description of the spatio-temporal frequency characteristics of the SCi layers, the layers serving as the origin of the ascending tectofugal sensory-motor system that transmits multisensory information to the basal ganglia of the amniotic brain [58].

2.6. Subcortical loops through the basal ganglia

Anatomical evidence suggests that many subcortical structures having the capacity to guide movements also have connections with the basal ganglia, besides the cortical connections. These subcortical connections are best conceived of as a series of parallel, at least partially closed, loops. In addition to its sensorimotor connections, the SC is one of the principal targets of both major output nuclei of the basal ganglia (the internal globus pallidus and the SN pars reticulata – SNr) [59-63]. These connections are considered to be the principal routes whereby information processing within the basal ganglia influences brainstem motor mechanisms, particularly in the context of oculomotor control [64]. It is significant that ascending projections from the SC specifically target regions of the thalamus that provide the major thalamic input to the two principal input structures of the basal ganglia (the striatum and the subthalamic nucleus) [65-67]. This arrangement suggests that the SC is an important afferent source of both sensory and motor information, in addition to a principal recipient of basal ganglia output. In this particular case, the input–output relationships are best characterized as several possibly independent, but overlapping, closed-looped systems [68].

2.6.1. The superficial layer–extrageniculate visual thalamic loop

The major ascending output of the exclusively visual SCs layers is directed to the extrageniculate visual thalamus (the LP-Pul) [10;69;70]. In addition to its connections with the extrastriate visual cortex [71;72], this thalamic region also projects extensively to the

lateral aspects of the body and tail of the CN and dorsolateral putamen [66;70;73]. The relay in the lateral posterior thalamus provides a route by which subcortical visual input can be made directly available to the striatum. In the next link of the loop, the 'direct' striatonigral projection topography ensures that visual information associated with input from the lateral posterior thalamus would be directed preferentially to the lateral aspects of the SNr and to the SN pars lateralis (SNl) [68]. It is within these nigral regions that signals related to visual orienting are most frequently encountered [74], and from which the final return link of the visual loop back to the superficial layers (and possibly to the deeper collicular layers) originates [61].

2.6.2. The deep layer–intralaminar and posterior thalamic loops

Ascending projections from the SCi terminate mainly in regions of the thalamus that give rise to significant afferent projections to the basal ganglia input nuclei. According to one approach these thalamic nuclei are the caudal intralaminar complex (centromedian and parafascicular nuclei) and the rostral intralaminar thalamic group (central lateral, paracentral and central medial nuclei) [75;76]. However, based on the results of other research groups and also our own laboratory, projections from the SCi also terminate in the posterior extrageniculate thalamus, mostly in the Sg [70;77]. Given that both the caudal and rostral intralaminar thalamic nuclei, as well as the Sg provide topographically ordered projections to all functional territories within the striatum [65;78], the colliculo-thalamo-basal ganglia-collicular projections involving these subregions of the intralaminar and posterior thalamus could represent components of functionally independent parallel loops.

Thus, in summary, there appear to be at least two, presumably closed subcortical looped systems through the basal ganglia arising from, and returning to, the SC [68].

Since the SC is connected to the basal ganglia through several pathways, and the SCi is strongly involved in processing multisensory information and multisensory integration, the main purpose of our experiments was to record and analyze the multisensory information processing and multisensory integration ability of the CN and the SN.

3. Aims of the study

The aims of our study were to examine and evaluate the role of the ascending tectofugal system and the connected basal ganglia in multisensory information processing, and thus, to provide further data regarding the function of this complex system in the neurological processes of the mammalian brain. The concrete aims of our experiments were the following:

- to compare the spatio-temporal spectral response properties in different structures of the ascending tectofugal system;
- to describe the sensory receptive field properties of neurons in the CN and the SN;
- to examine if there are any multisensory neurons within the basal ganglia;
- to check the modality distribution among the sensory neurons in the basal ganglia;
- to find out if there is parallel processing of the different sensory modalities or multisensory integration in the ascending tectofugal system;
- to investigate the multisensory cross-modal interactions within the basal ganglia.

4. Materials and methods

4.1. Animal preparation and surgery

Our experiments were performed on five to seven adult cats per experiment of either sex weighing between 2.8 and 3.5 kg. All experimental procedures were carried out so as to minimize the number and suffering of the animals involved and followed the European Communities Council Directive of 24 November 1986 (86 609 EEC) and the National Institute of Health guidelines for the care and use of animals for experimental procedures. The experimental protocol had been accepted and approved by the Ethical Committee for Animal Research of Albert Szent-Györgyi Medical and Pharmaceutical Center at the University of Szeged. The animals were initially anesthetized with ketamine hydrochloride (30 mg/kg i.m., Calypsol). A subcutaneous injection of 0.2 ml 0.1% atropine sulfate was administered preoperatively, to reduce salivation and bronchial secretion. The trachea and the femoral vein were cannulated and the animal was placed in a stereotaxic head holder. In case of the experiments concerning the multisensory information processing the animal's head was fixed to a vertical metal bar with the aid of acrylate and the ear-bars were removed. All wounds and pressure points were routinely infiltrated with local anesthetic (procaine hydrochloride, 1%). During the surgical procedure, the anesthesia was continued with halothane (1.6%, Fluothane) in air. The animal was initially immobilized with gallamine triethiodide (20 mg/kg, Flaxedyl). During recording sessions, a liquid containing gallamine triethiodide (8 mg/kg/h), glucose (10 mg/kg/h) and dextran (50 mg/kg/h) in Ringer lactate solution was infused at a rate of 4 ml/h. Atropine sulfate (1–2 drops, 0.1%) and phenylephrine hydrochloride (1–2 drops, 10%) were administered locally to dilate the pupils and block accommodation and to retract the nictitating membranes, respectively. The eye contralateral to the recording site was equipped with a +2.0 diopter contact lens. The ipsilateral eye was covered during the visual stimulation and recordings. Throughout the experiments, anesthesia was maintained with a gaseous mixture of air and halothane (0.8–1.0%). The depth of anesthesia was monitored by continuous reading of the end-tidal halothane values and by repeated checks of the electroencephalogram and electrocardiogram. There was continuous high-amplitude, low-

frequency electroencephalogram activity with sleep spindles and we also checked repeatedly whether any interventions or a forceful pressing of the forepaws could induce desynchronization. The minimum alveolar anesthetic concentration (MAC) values calculated from the end-tidal halothane readings always lay in the range given by Villeneuve and Casanova [79]. The end-tidal halothane concentration, the MAC values and the peak expired CO_2 concentrations were monitored with a capnometer. The peak expired CO_2 concentration was kept within the range of 3.8–4.2% by adjusting the respiratory rate or volume. The heart rate and O_2 saturation in the capillary blood were monitored by electrocardiography and pulse oxymetry. The body temperature of the animal was maintained at around 37°C via a warm-water heating blanket with automatic control. The skull was opened with a dental drill to allow a vertical approach to the appropriate brain structures. The dura mater was removed and the cortical surface was covered with a 4% solution of 38°C agar dissolved in Ringer's solution. The retinal landmarks and major retinal blood vessels were projected routinely onto a tangent screen, twice a day, using a fiber optic light source [80]. The area centralis was plotted by reference to the optic disc (14.6° medially and 6.5° below the center of the optic disc) [81].

4.2. Recording

Extracellular single-cell recordings were performed in the SCi, the CN and the SN with tungsten microelectrodes (A-M Systems, Inc., USA) with an impedance of 2-4 MΩ. Vertical penetrations were performed within Horsley-Clarke coordinates anterior 1 to 4, lateral 2 to 6 in the stereotaxic depths from 11 to 15 in case of the SCi, while, to record CN and SN single units the positions of the recording sites were between the Horsley-Clarke co-ordinates anterior 12–16; lateral 4–6.5 at the stereotaxic depths between 12 and 19 mm, and anterior 3–6; lateral 4–6 at the stereotaxic depths between 4 and 7 mm, respectively. The microelectrodes were advanced with a microstepper. Action potentials were conventionally amplified, displayed on an oscilloscope and transformed through a loudspeaker. The extents of the visual receptive fields were estimated subjectively by listening to the responses of the single units to the movements of a hand-held lamp.

4.3. Spatio-temporal visual stimulation

In case of the spatio-temporal visual stimulation of the SCi neurons, an 18-inch computer monitor (refresh rate, 85 Hz) was placed 42.9 cm in front of the animal. The diameter of the stimulation screen was 22.5 cm, and the cat therefore saw it in 30 deg. The mean luminance of the screen was 23 cd/m^2. For studies of the spatiotemporal characteristics of the cells, high-contrast (96%), drifting sinewave gratings were used. The sinusoidal gratings were moved along four different axes in eight different directions (0-315 deg at 45 deg increments) to find the optimal moving direction of each unit. The optimal direction of each unit was further used to describe its spatial and temporal characteristics. The tested spatial frequencies ranged from 0.025 to 0.95 cycle/deg (c/deg) and the temporal frequencies from 0.07 to 33.13 cycles/s (Hz). Stimuli were presented in a pseudo-random sequence in a series consisting of eight spatiotemporal frequency combinations of moving gratings. Each spatiotemporal frequency combination was presented at least 12 times. The interstimulus interval was consistently 1 s.

4.4. Visual, auditory, somatosensory and multisensory stimulation

In case of investigating the multisensory information processing abilities of the neurons in the CN and the SN, we applied visual, auditory, somatosensory and multisensory stimulations. For visual stimulation, light spots of 1° to 10° in diameter were generated by a projector device equipped with an adjustable slit-lamp diaphragm. The stimuli were moved with a computer-controlled moving mirror system and were projected across the tangent screen (52 cm in front of the animal) in the optimal moving direction and at an optimal velocity (30–120°/s) for each unit. The duration of the stimulus movement was 1 s. The auditory stimulation applied to investigate the extents of the auditory receptive fields was white noise. The sound intensity was constantly 60 dB. The duration of the auditory stimulation was 1 s. We estimated the extents of the binaural auditory receptive fields in the horizontal plane. Computer-controlled loudspeakers were placed throughout the whole 360° azimuth of the horizontal plane and the neuronal responses to all stimulus locations were recorded in 45° steps. The width of the auditory

receptive field of a neuron was determined by the locations of stimuli that induced significant responses. Somatosensory stimulation was achieved with the motion of a computer-controlled pen driver whose tip was attached to nylon fibers. The surface area of the stimulator was 1 cm^2. The stimulator provided light mechanical stimulation of different parts over the whole skin of the animal. The duration of a somatosensory stimulation was also 1 s. The computer-controlled stimuli were presented in a pseudo-random order, either separately (visual or auditory or somatosensory) or simultaneously in bimodal (visual-auditory, visual-somatosensory or auditory-somatosensory) or trimodal (visual-auditory-somatosensory) combinations. Whenever a single unit was found that was visually or auditory or somatosensory sensitive, at least 10 trials were run in each condition. The interstimulus interval was consistently 1 s.

4.5. Data analysis and examination of the multisensory integration

Individual action potentials were distinguished with the help of a spike-separator system (SPS-8701, Australia). The number and temporal distribution of the action potentials recorded during stimulation were stored as peristimulus time histograms (PSTHs, 10 ms bin) and analyzed off-line. Every statistical analysis mentioned in the thesis has been carried out by the Statistica® software. The duration of the prestimulus time (during which the background activity of the neuron was recorded to a stationary stimulus) was 1000 ms, similarly to the peristimulus time (during which a moving stimulus was shown). The net discharge rate, calculated as the difference between the mean firing rates of the cell obtained during stimulus movement and the background activity corresponding to the mean activity during the 200 ms preceding the movement in the prestimulus period, was used to characterize the response amplitude of the SCi, CN and SN neurons.

A multisensory cross–modal interaction was considered to exist when the difference between the net firing rate of the most effective single modality and the bimodal or trimodal peristimulus firing rate proved to be significant by the analysis of variance (ANOVA, $p<0.05$; [82]). To quantify the strengths of the facilitatory interactions, the percentage enhancements were calculated via the formula coined by Meredith and Stein [14]:

$$\text{Percentage enhancement} = 100 \times (CM - SM_{max})/SM_{max}.$$

To quantify the strengths of the inhibitory interactions and enable comparisons with the percentage enhancement, we introduced the formula:

$$\text{Percentage inhibition} = 100 \times (SM_{max} - CM)/CM.$$

In both formulae CM is the mean number of net impulses evoked by the bimodal stimulus and SM_{max} is the mean number of net impulses evoked by the most effective single-modality stimulus. In case of the latter formula, an inhibition percentage equal to 100% does not mean complete abolition of the unimodal response; thus, the inhibition percentage values derived from this formula can be higher than 100%. An inhibition percentage equal to 100% means a 50% decrease in the unimodal activity, while an inhibition percentage equal to 200% means a decrease in the unimodal activity to one-third during multisensory stimulation.

4.6. Histological control

At the end of the experiments, the animals were deeply anaesthetized with sodium pentobarbital (200 mg/kg i.v.) and transcardially perfused with 4% paraformaldehyde solution. The brains were removed, cut into coronal sections of 50 μm and stained with Neutral Red. Electrolytic lesions marked the locations of successful electrode penetrations. The recorded sensory neurons were located in the SCi, the dorsolateral aspect of the CN and in the SNr.

5. Results

5.1. Comparison of the spatio-temporal spectral response profiles in the ascending tectofugal system

We compared the spatio-temporal spectral receptive field properties of the SCs, the SCi, the Sg and the CN using a one-way ANOVA analysis. The paired comparison of the individual structures was performed by Tukey post-hoc analysis.

The mean optimal spatial frequency was 0.10±0.01 c/deg (N=72 range: 0.03–0.47 c/deg) in the SCs, 0.06±0.02 c/deg (N=99, range: 0.025–0.3 c/deg) in the SCi, 0.05±0.04 c/deg (N=105, range: 0.025–0.24 c/deg) in the Sg and 0.05±0.03 c/deg (N=89, range: 0.025–0.18 c/deg) in the CN. The summarized statistical analysis of the investigated structures revealed a significant difference among the optimal spatial frequencies of the investigated structures ($p<0.001$, $F_{(3,\ 374)}=16.376$). The post-hoc analysis showed that the mean optimal spatial frequency measured in the SCs was significantly higher than that of the SCi ($p<0.001$), the Sg ($p<0.001$) and the CN ($p<0.001$). In contrast to this, we found no significant difference ($p>0.05$) among the optimal spatial frequencies in the SCi, the Sg and the CN (Fig. 1A).

The mean spatial frequency bandwidth of the neurons having spatial band-pass characteristics (in case of these neurons, there was an attenuation of the response to at least half the height of the maximum when stimulated with lower or higher spatial frequencies than the optimal) was 1.84±0.15 octaves (N=35, range: 0.39–3.60 octaves) in the SCs, 1.06±0.56 octaves (N=24, range: 0.1–2.18 octaves) in the SCi, 1.07±0.69 octaves (N=41, range: 0.11–2.81 octaves) in the Sg and 1.31±0.76 octaves (N=15, range: 0.37–3.0 octaves) in the CN. Similarly to the optimal spatial frequency the summarized statistical analysis of the spatial frequency bandwidths revealed a significant difference among the investigated structures ($p<0.001$, $F_{(4,\ 236)}=6.317$). The post-hoc analysis showed that the spatial frequency bandwidth of the band-pass neurons in the SCs was significantly higher than that of the SCi ($p=0.004$), the Sg ($p<0.001$) and the CN ($p=0.006$). We found no significant difference ($p>0.05$) among the spatial frequency bandwidths of the SCi, the Sg and the CN (Fig. 1B).

The mean optimal temporal frequency was 6.84±0.71 c/s (N=62, range: 0.74–26.41 c/s) in case of the SCs, 9.06±5.49 c/s (N=99, range: 1.71–31.93 c/s) in the SCi, 8.53±4.43 c/s (N=105, range: 0.07–26.41 c/s) in the Sg and 10.6±4.8 c/s (N=89, range: 4.6–27.6 c/s) in the CN. The summarized statistical analysis of the investigated structures revealed a significant difference among the optimal temporal frequencies of the investigated structures ($p=0.04$, $F_{(3, 314)}=2.807$). The post-hoc analysis showed that the mean optimal temporal frequency in the SCs was significantly lower than that of the SCi ($p=0.023$), the Sg ($p=0.012$) and the CN ($p=0.038$). In contrast we found no significant difference ($p>0.05$) among the optimal temporal frequencies in the SCi, the Sg and the CN (Fig. 1C).

The mean temporal frequency bandwidth of the neurons having temporal band-pass characteristics (in case of these neurons, there was an attenuation of the response to at least half the height of the maximum when stimulated with lower or higher temporal frequencies than the optimal) was 2.38±0.22 octaves (N=42, range: 0.40–5.90 octaves) in the SCs, 2.32±0.97 octaves (N=48, range 0.25–4.29 octaves) in the SCi, 1.66±1.37 octaves (N=73, range: 0.03–7.91 octaves) in the Sg and 1.38±1.0 octaves (N=55, range: 0.09–5.36 octaves) in the CN. Similarly to the optimal temporal frequency, the summarized statistical analysis of the temporal frequency bandwidths revealed a significant difference among the investigated structures ($p<0.001$, $F_{(4, 307)}=13.797$). The post-hoc analysis showed that the temporal frequency tuning bandwidth of the neurons in the SCs and the SCi was not significantly different, but the temporal frequency bandwidths of both the SCs and the SCi neurons were significantly higher than that of the neurons in the Sg ($p<0.001$ in case of the SCs and $p<0.001$ in case of the SCi) and the CN ($p=0.023$ in case of the SCs and $p=0.03$ in case of the SCi). We found no significant difference ($p>0.05$) between the temporal frequency bandwidths of the Sg and the CN (Fig. 1D).

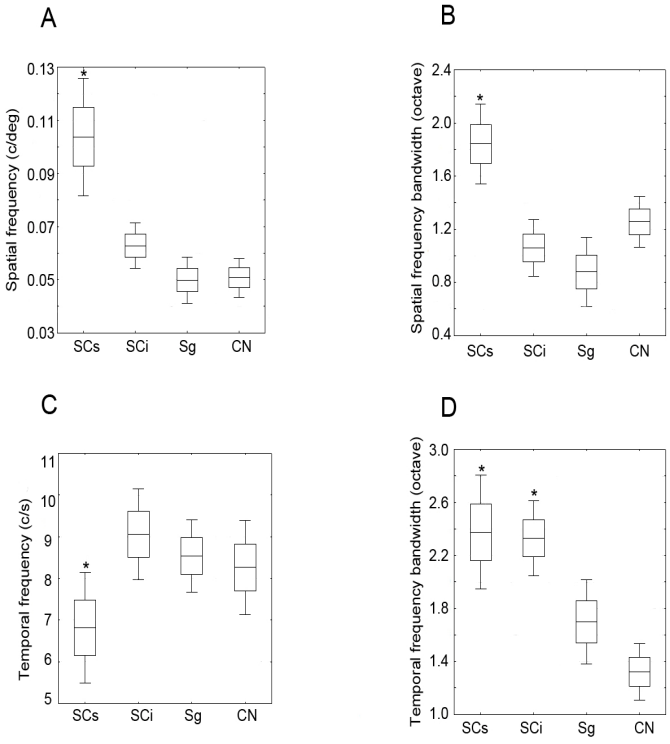

Figure 1. Comparison of the spatial and temporal frequency tuning properties in the ascending tectofugal system. **A**: Comparison of the mean optimal spatial frequencies. **B**: Comparison of the spatial frequency bandwidths. **C**: Comparison of the mean optimal temporal frequencies. **D**: Comparison of the temporal frequency bandwidths. Stars denote significant differences between the analyzed structures.

5.2. Visual, auditory and somatosensory receptive field properties of neurons in the basal ganglia

Altogether 302 single neurons in the CN and 480 single neurons in the SNr were recorded; 111 of these CN units and 124 of the nigral neurons exhibited excitatory responses to visual and/or auditory and/or somatosensory stimulation. We analyzed the responses of a total of 77 CN and 75 SNr excitatory responsive single neurons to separate visual, auditory or somatosensory stimulus presentations and after that, to multisensory stimulation in detail.

The unimodal neurons reacted only to visual or auditory or somatosensory stimulation. From the recorded CN neurons 46 showed visual sensitivity. Most of the recorded units were located between the Horsley-Clark co-ordinates anterior 12–13 and lateral 4–6.5, although some visual units were recorded at anterior 14 and 15, too. Visually responsive units were confined to the dorsolateral part of the CN. We could not detect visually responsive CN units in its more anterior part (anterior 16 and 17).

From the recorded SNr neurons, 49 were found to be visually responsive. Histological control of the recording tracks revealed that all the 49 units were located in the SNr. The visually responsive neurons were located between Horsley-Clark co-ordinates anterior 3–6 and lateral 3–6. We could not record excitatory visual activity in any other part of the SN. We determined the location and size of the receptive fields of the neurons with the help of a hand-held lamp, by listening to the amplified neuronal electrical responses to visual stimulation through a loudspeaker. Similarly to earlier findings, our subjective estimation of the extents of the visual receptive fields demonstrated that the visual receptive fields were extremely large: they covered a major part of the contralateral hemifield and extended deep into the ipsilateral hemifield, yielding a receptive field that overlapped almost totally with the visual field of the contralateral eye [83]. No signs of retinotopy were observed.

We found 40 neurons in the CN and 50 neurons in the SNr that responded to somatosensory stimulation. The extents of the somatosensory receptive fields were large. They seemed to cover the whole contralateral and ipsilateral body surface and the whiskers of the animal. We could not detect somatotopic organization within the CN and the SNr.

Only a small proportion of the neurons displayed auditory sensitivity (26 neurons in the CN and 24 neurons in the SNr, respectively). The auditory neurons in the CN and the SNr were consistently binaural and possessed extremely large receptive fields. Single auditory neurons processed auditory information from the whole 360° azimuth of the horizontal plane.

5.3. Multisensory response properties of neurons in the basal ganglia

The bimodal neurons were responsive to two different sensory modalities. We found visual-auditory, visual-somatosensory and auditory-somatosensory neurons in the basal ganglia. The trimodal neurons responded significantly to all three sensory modalities

tested. Fifty (65%) of the sensory CN neurons exhibited a unimodal character, reacting to only one investigated modality, while a smaller proportion (27, 35%) of them were multisensory, reacting to two or three different sensory modalities (7 visual-auditory, 9%; 9 visual-somatosensory, 12%; 3 auditory-somatosensory, 4% and 8 trimodal neurons, 10%). A majority of the sensory neurons recorded in the CN responded to visual or somatosensory stimulation. Similarly to the unimodal units, the sensory receptive fields of the multisensory CN neurons were extremely large, covering the whole of the approachable sensory field, i.e. a single trimodal CN neuron could process sensory information from the whole visual field of the contralateral eye, from the loudspeakers located throughout the whole 360° azimuth and from the whole body surface of the animal (Fig. 2A).

Thirty-eight (51%) of the 75 SNr units exhibited a unimodal character while the remaining 37 (49%) units were multisensory (5 visual-auditory, 7%; 16 visual-somatosensory, 21%; 5 auditory-somatosensory, 7%; 11 trimodal neurons, 14%). Similarly as for the unimodal SNr units, the receptive fields of the multisensory nigral neurons were extremely large (Fig. 2B).

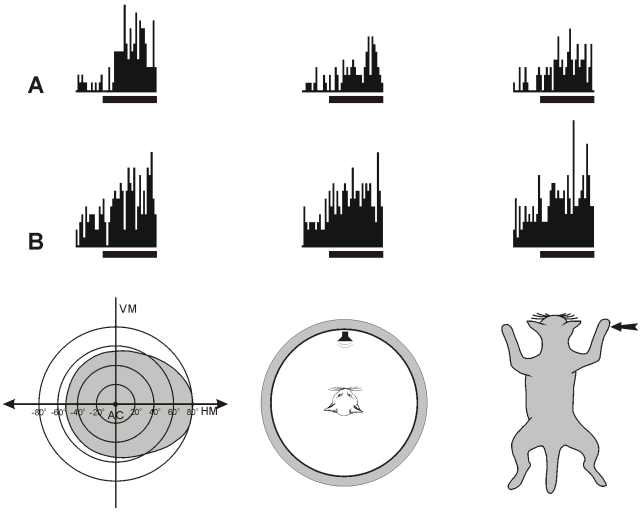

Figure 2. Responses of (A) one trimodal caudate neuron and (B) one trimodal nigral neuron to visual (left side), auditory (middle) and somatosensory (right side) stimulation. The shaded areas below indicate the extents of the receptive fields and the sites of stimulation. The peristimulus time histograms show the single-unit activities before and during (indicated by thick black lines) stimulation. The black lines represent the duration of the stimulation of 1 s.

5.3.1. Multisensory integration in the basal ganglia

The multisensory integration abilities of the 77 CN and 75 SNr sensory single-neurons were analyzed in detail. To exclude the differences in multisensory integration of single-neurons related to spatial variations, we attempted to make consistent use of the same stimulation sites throughout the whole study.

5.3.2. Significant facilitatory and inhibitory interactions in the caudate nucleus and the substantia nigra

We found that 36 of the 77 investigated CN neurons (47%) and 41 of the 75 SNr neurons (55%) exhibited significant multisensory cross-modal interactions.

We analyzed altogether 36 interactions between the CN units and 39 interactions between the SNr neurons. The large majority of the interactions in both structures were multisensory response enhancements (26/36, 72% in the CN and 28/39, 72% in the SNr) and approximately one quarter of them were multisensory response depressions (10/36, 28% in the CN and 11/39, 28% in the SNr). We found significant facilitatory and inhibitory interactions in both structures in each multisensory stimulus combination tested (multisensory interactions in case of 2/36 [6%] visual-auditory, 8/36 [22%] visual-somatosensory, 6/36 [17%] auditory-somatosensory and 20/36 [55%] trimodal CN neurons; and in case of 2/39 [5%] visual-auditory, 16/39 [41%] visual-somatosensory, 2/39 [5%] auditory-somatosensory and 19/39 [49%] trimodal SNr neurons) (Fig. 3 and 4).

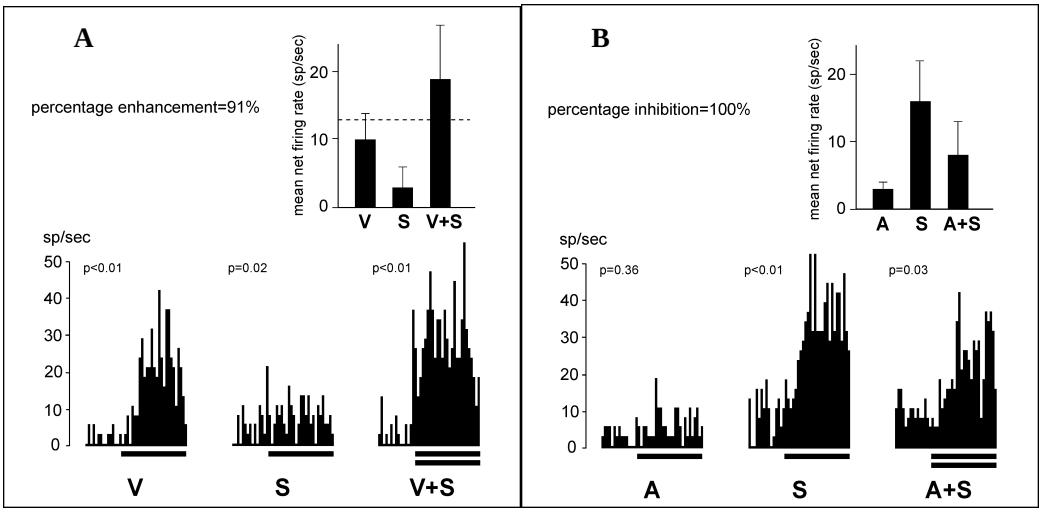

Figure 3. Multisensory response enhancement (A) and depression (B) in a caudate nucleus neuron. A: The left PSTH demonstrates the neuronal response to visual (V), the middle one to somatosensory (S) and the right one to combined visual-somatosensory (V + S) stimulation. The p-value above each PSTH denotes the significance level of the response. Each PSTH shows the single-unit activities before and during (indicated by thick black lines) stimulation. The thick black lines indicate a stimulation interval of 1000 ms. The calibration denotes the firing rates (sp/sec). Note that the converging inputs from the different sensory modalities produced dramatic changes in the activity of this unit. The columns on the right side of the figure are proportionate to the mean net firing rate of this unit to visual (V), somatosensory (S) and bimodal (V + S) stimulation. The error bars denote standard deviations. The response of this unit to multisensory stimulation is notably stronger than the sum of the unimodal responses indicated by the broken line. **B**: The left PSTH demonstrates the neuronal response to auditory (A), the middle one to somatosensory (S) and the right one to combined auditory-somatosensory (A + S) stimulation. The conventions are the same as for part A. Note that the converging inputs from the different sensory modalities produced a dramatic decrease in the activity of this unit. The columns on the right side of the figure are proportionate to the mean net firing rate of this unit to auditory (A), somatosensory (S) and bimodal (A + S) stimulation.

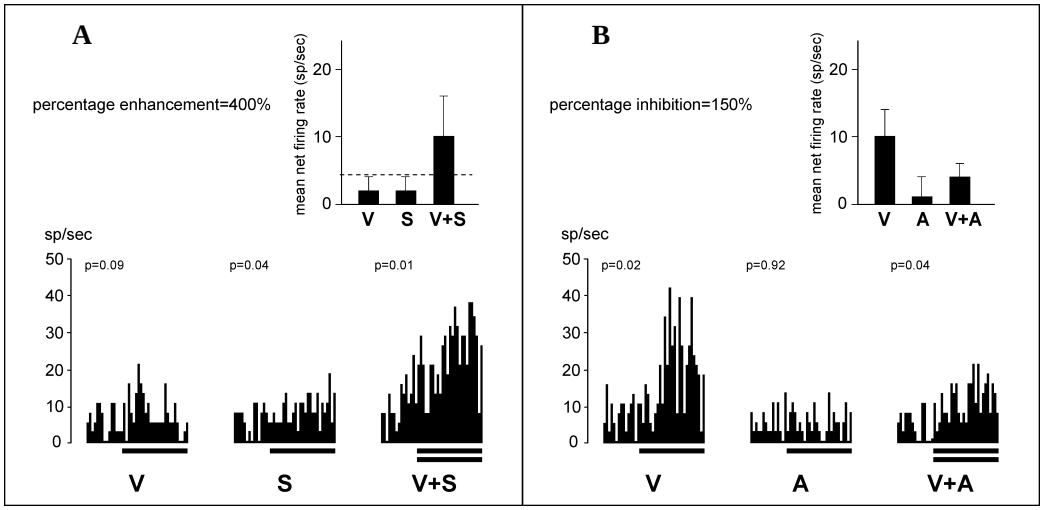

Figure 4. Multisensory response enhancement (A) and depression (B) in a substantia nigra neuron. A: The left PSTH demonstrates the neuronal response to visual (V), the middle one to somatosensory (S) and the right one to combined visual-somatosensory (V + S) stimulation. The conventions are the same as on Fig. 3. Both unimodal stimulus presentations elicited slight responses, but the converging inputs from the different sensory modalities produced dramatic changes in the activity of this unit. **B**: The left PSTH demonstrates the neuronal response to visual (V), the middle one to auditory (A) and the right one to combined visual-auditory (V + A) stimulation. The conventions are as for Fig. 3. This unit elicited a vigorous response to unimodal visual stimulation, but was only very weakly responsive to auditory stimulation, while the almost ineffective auditory stimulus combined with the visual one produced a dramatic decrease in the neuronal activity.

5.3.3. Magnitude of the multisensory interactions in the caudate nucleus and the substantia nigra

We found slightly stronger facilitatory and inhibitory multisensory interactions in the CN than in the SNr. Despite this, there was no significant difference (Mann-Whitney U-test, p=0.15) between the strengths of the facilitatory interactions in the CN (median=148%, N=26, range 44–625%) and the SNr (median=115%, N=28, range 40–574%). Similarly, there was no significant difference (Mann-Whitney U-test, p=0.22) between the strengths of the inhibitory interactions in the CN (median=161%, N=10, range 37–688%) and the SNr (median=126%, N=11, range 41–391%). Comparison of the

strengths of the overall inhibitory and excitatory interactions between the CN (median=140%, N=36, range: 37–688%) and the SNr (median=116%, N=39, range 40–574%) demonstrated no significant difference (Mann-Whitney U-test, p=0.21) (Fig. 5).

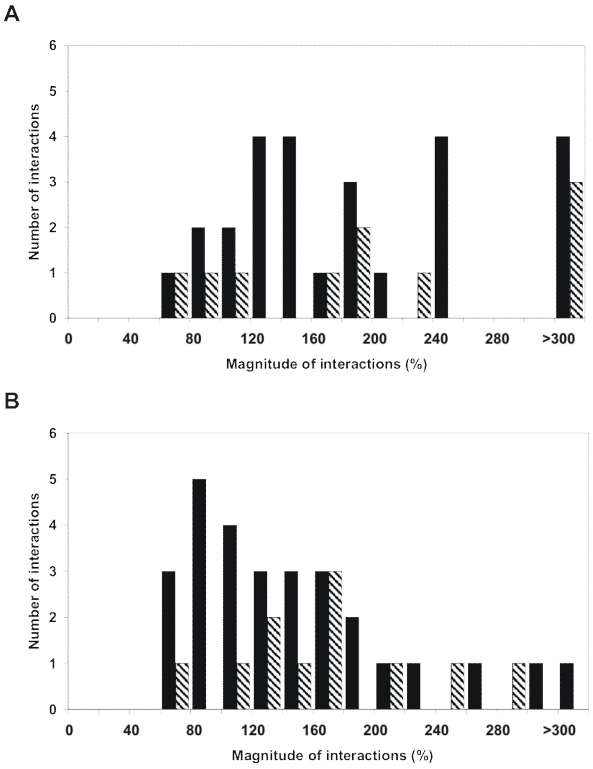

Figure 5. Distribution of the multisensory indices in the caudate nucleus (A) and in the substantia nigra (B). The black columns denote the percentage enhancement, and the striped columns denote the magnitude of the multisensory response depression. The abscissa reflects the magnitude of multisensory interactions (%), and the ordinate the numbers of interactions.

5.3.4. Subadditive, additive and superadditive multisensory interactions in the caudate nucleus and the substantia nigra

Stanford et al. (2005) [84] introduced a different way to quantify multisensory interactions in the SC. They reported subadditive, additive and superadditive response enhancement effects as concerns the relation of multisensory discharge rates to the magnitude of the unimodal responses. The classification was a subadditive interaction when the multisensory response was shown by a t-test to be significantly lower than the sum of the two different unimodal responses, an additive interaction when the bimodal response was not different from the sum of the unimodal responses, and a superadditive interaction when the multisensory response was significantly higher than the sum of the unimodal responses. We also analyzed the interactions in the CN and the SNr in a similar

way. Ten of the 26 (38%) facilitatory interactions found in the CN and 15 of the 28 (54%) in the SNr were superadditive (t-test, $p<0.05$). However, the remaining 16 (62%) facilitatory interactions in the CN and 13 (46%) in the SNr were additive (t-test, $p>0.05$). In contrast, the above-mentioned ten (100%) multisensory response depressions in the CN and 11 (100%) in the SNr were consistently subadditive, the multisensory net discharge rate being significantly lower than the sum of the net unimodal responses (t-test, $p<0.05$).

5.3.5. Inverse effectiveness principle in the caudate nucleus and the substantia nigra

In both the CN and the SNr, we investigated the correlation between the magnitudes of the best unimodal responses and the magnitudes of the response enhancements (percentage enhancements; [14]). The inverse effectiveness principle was observed in both structures, i.e. the cells with the weakest net unimodal responses exhibited the strongest enhancement effects. There was a strong significant negative correlation between the strengths of the best unimodal net responses and the percentage enhancements in the CN ($N=26$, $r=-0.52$, $p<0.01$) and also in the SNr ($N=28$, $r=-0.39$, $p<0.01$).

5.4. Sensory modality distribution in the basal ganglia

5.4.1. A majority of the caudate nucleus and substantia nigra units seem to be unimodal in the separate single modality tests

The classification based only on the significant responses of the CN and SNr neurons to the separate sensory modalities demonstrated that a majority of the CN (50/77, 65%) and SNr (38/75, 51%) neurons seemed to be unimodal, reacting to a statistically significant extent to only one of the investigated modalities, and only a smaller proportion of the units exhibited a multisensory character (27/77, 35% in the CN and 37/75, 49% in the SNr), reacting to a statistically significant extent to two or three different sensory modalities (Table 1 and 2).

Modality	A	B
Unimodal	50 (65%)	**25 (32%)**
Visual	22 (29%)	**10 (13%)**
Auditory	8 (10%)	**4 (5%)**
Somatosensory	20 (26%)	**11 (14%)**
Multisensory	27 (35%)	**52 (68%)**
Visual-auditory	7 (9%)	**9 (12%)**
Visual-somatosensory	9 (12%)	**14 (18%)**
Auditory-somatosensory	3 (4%)	**10 (13%)**
Trimodal	8 (10%)	**19 (25%)**
Altogether	77 (100%)	**77 (100%)**

Table 1. Modality distribution of sensory neurons in the caudate nucleus. A: Modality distribution of the CN neurons in separate sensory modality tests without multisensory stimulus combinations. **B**: Modality distribution of the CN neurons when multisensory combinations and multisensory interactions were also analyzed. Note the much higher number of multisensory units when multisensory integration was also analyzed. Thus, the separate sensory modality tests without the analysis of multisensory responses may strongly underrepresent the number of multisensory units in the CN.

Modality	A	B
Unimodal	38 (51%)	**15 (20%)**
Visual	17 (23%)	**5 (7%)**
Auditory	3 (4%)	**0 (0%)**
Somatosensory	18 (24%)	**10 (13%)**
Multisensory	37 (49%)	**60 (80%)**
Visual-auditory	5 (7%)	**6 (8%)**
Visual-somatosensory	16 (21%)	**19 (25%)**
Auditory-somatosensory	5 (7%)	**5 (7%)**
Trimodal	11 (14%)	**30 (40%)**
Altogether	75 (100%)	**75 (100%)**

Table 2. Modality distribution of sensory neurons in the substantia nigra. A: Modality distribution of the SNr neurons in separate sensory modality tests without multisensory stimulus combinations. **B**: Modality distribution of the SNr neurons when multisensory combinations and multisensory interactions were also analyzed. Note the much higher number of multisensory units when multisensory integration was also tested. Thus, the separate sensory modality tests without the analysis of multisensory responses may strongly underestimate the number of multisensory units in the SNr.

5.4.2. Is unimodal clearly unimodal? Or is it after all multisensory in some cases?

In order to analyze the multisensory information-processing abilities of the same 77 CN and 75 SNr neurons, we also recorded the neuronal responses of these units to multisensory stimulus combinations. We found that 36 of the 77 investigated CN neurons (47%) and 41 of the 75 SNr neurons (55%) exhibited significant multisensory cross-modal interactions. Surprisingly, only 11 of these 36 CN and 18 of these 41 SNr integrative cells had been defined as multisensory in the separate single modality tests, i.e. these units responded to a statistically significant extent to at least two different sensory modalities presented alone. In contrast, a larger proportion of the integrative CN and SNr units responded in a separate modality test to only one sensory modality, and thus these units were classified as unimodal on the basis of the results of the separate single modality tests. Twenty-five of the 36 integrative CN cells (12 visual, 3 auditory and 10 somatosensory) and 23 of the 41 integrative SNr units (12 visual, 3 auditory and 8 somatosensory) with a significant cross-modal interaction had responded to a statistically significant extent only to individual auditory or visual or somatosensory stimulation, but the originally ineffective modality or modalities were able to induce multisensory interactions. Ten of the 25 CN units that were classified earlier as unimodal displayed a significant multisensory interaction with only one ineffective modality presented together with the effective stimulus, i.e. these units seemed to be bimodal. The other 15 units must be classified as trimodal, because 10 of these cells exhibited interactions with both ineffective modalities or exhibited facilitatory interactions only on trimodal stimulus presentation. Similarly, 8 of the 23 SNr units classified earlier as unimodal demonstrated an interaction with only one ineffective modality, while the other 15 neurons were trimodal in the sense that 11 cells revealed interactions with both ineffective modalities and 4 units displayed facilitatory interactions only on trimodal stimulus presentation. Thus, despite the consistent results of the neuronal responses to separate sensory stimulations, these 25 CN and 23 SNr units seem to be multisensory. We define a neuron as multisensory either when it reacts to two or three different sensory modalities to a statistically significant extent (Fig. 6A and 7A), or when it reacts to only one sensory modality to a significant extent, but at least one of the ineffective modalities induced a multisensory cross-modal interaction (Fig. 6B and 7B). Thus, a majority of the investigated CN (52/77, 68%) and SNr (60/75, 80%) units proved

to be of a multisensory character, and only a smaller proportion of them (25/77, 32% in the CN, and 15/75, 20% in the SNr) were classified as absolutely unimodal (Table 1 and 2). We compared the modality distribution in the CN and the SNr and we found that there's a significant difference between the modality distributions in the two structures (Pearson Chi-square test: χ^2 =16.95; df=6; p<0.01).

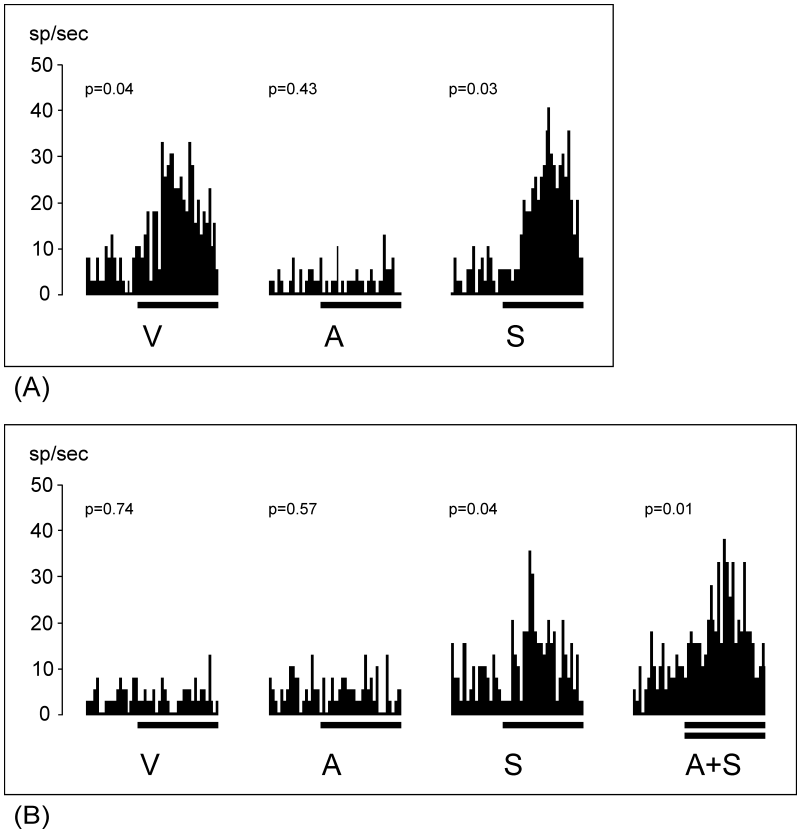

Figure 6. Multisensory responses of two caudate nucleus neurons. A: Responses of a multisensory CN neuron that responded significantly to both visual and somatosensory stimulation in the separate single modality tests. The left PSTH demonstrates the neuronal response to visual (V), the middle one to auditory (A) and the right one to somatosensory (S) stimulation. **B**: Responses of a multisensory CN neuron that responded significantly to only somatosensory stimulation in the separate single modality tests, but the ineffective auditory stimulus presented simultaneously with the somatosensory stimulus induced a significant multisensory response enhancement. The left PSTH demonstrates the neuronal response to visual (V), the second one to auditory (A), the third one to somatosensory (S) and the right one to combined auditory-somatosensory (A+S) stimulation. The p value above each PSTH denotes the significance level of a response. Each PSTH shows the single-unit activities before and during (indicated by thick black lines) stimulation. The thick black lines indicate a stimulation interval of 1000 ms. The calibration denotes the firing rates (sp/sec).

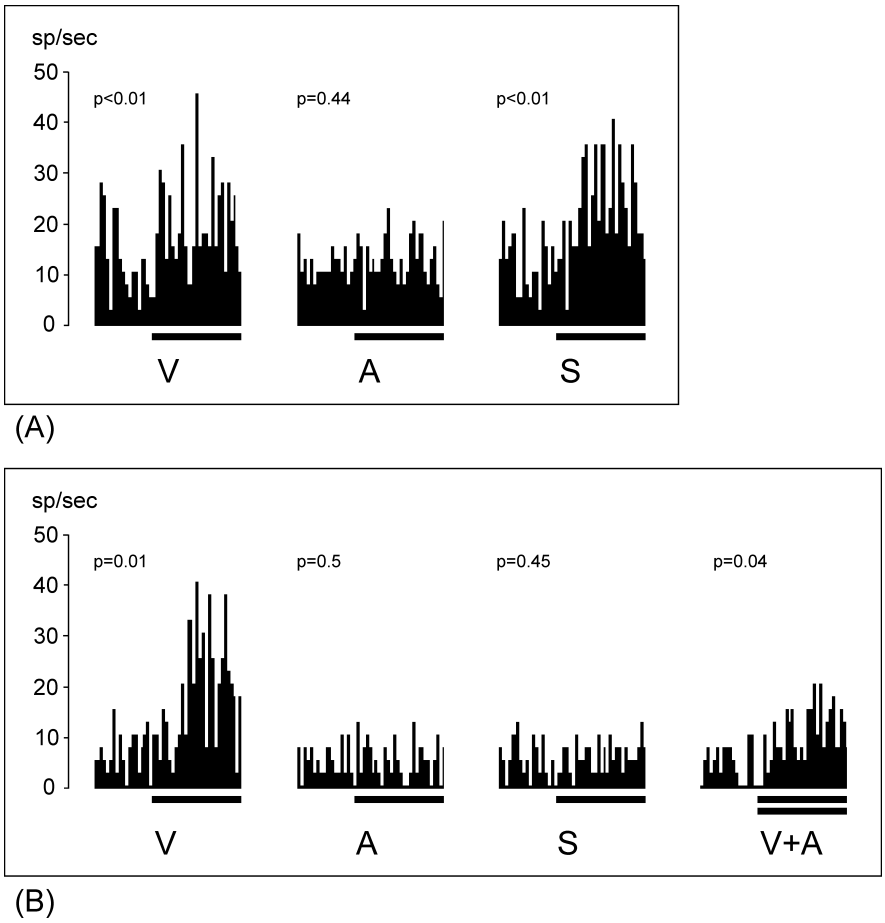

Figure 7. Multisensory responses of two substantia nigra neurons. A: Responses of a multisensory SNr neuron that responded significantly to both visual and somatosensory stimulation in the separate single modality tests. The left PSTH demonstrates the neuronal response to visual (V), the middle one to auditory (A) and the right one to somatosensory (S) stimulation. **B**: Responses of a multisensory SNr neuron that responded significantly to only visual stimulation in the separate single modality tests, but the ineffective auditory stimulus presented simultaneously with the visual stimulus induced a significant multisensory response depression. The left PSTH demonstrates the neuronal response to visual (V), the second one to auditory (A), the third one to somatosensory (S) and the right one to combined visual-auditory (V+A) stimulation. The conventions are the same as on Fig. 6.

6. Discussion

6.1. Spatio-temporal spectral response profiles in the ascending tectofugal system

6.1.1. Spatial frequency characteristics of different structures in the ascending tectofugal system

A large number of earlier studies focused on the description of the responsiveness of the visual neurons in the SC, the Sg and the CN merely to simple geometric forms, i.e. moving light spots and bars. These studies were therefore inappropriate to determine the responsiveness of these neurons to extended visual stimuli. Accordingly, our aim was to describe the spectral, spatio-temporal filter properties of the visually responsive neurons in the SCi, the Sg and the CN, and to suggest their role in the control of visuomotor actions.

The neurons located in the SCs responded optimally to very low spatial frequencies and displayed low spatial resolution [85]. Similar properties have been observed in the SCi. These findings indicate that the neurons in both the superficial and the intermediate SC layers act as good spatial filters in the low spatial frequency domain. The spatial frequency properties found in the SC resemble the functional properties of the W- and Y-type neurons in the LGNd [86-88], the Sg and the CN of the feline brain. Moreover, the lateral suprasylvian cortices: the PMLS [89;90], the anteromedial lateral suprasylvian area (AMLS; [91]), the AES cortex [92] and the neurons in area 21b (A21b) [93] also prefer very low spatial frequencies. However, the mean optimal spatial frequency and spatial resolution of the recorded SCi, Sg and CN neurons were much lower than those of the X-type neurons in the LGN [86;88], area 17 (A17), in which X input predominates [94-96], and the neurons in area 21a (A21a) [97;98].

The band-pass SCs neurons are moderately tuned to spatial frequencies [85], while the neurons in the intermediate layers show very narrow spatial frequency tuning. The mean spatial frequency tuning width of the superficial band-pass collicular neurons is comparable to those of the cortical visual areas A17, A18, A19, A21a and A21b, the PMLS and the LP-Pul of the thalamus [90;93;96;98-100], but much higher than those of the AES cortex [92], the Sg and the CN. In contrast, the mean tuning width found in the SCi is comparable to those of the AES cortex [92], the Sg and the CN, structures that

receive a tectal source of visual information from the intermediate and deep collicular layers.

We performed a concrete comparison of the mean optimal spatial frequency and the spatial frequency bandwidth values of the SCs, the SCi, the Sg and the CN, and we found that the neurons located in the SCs preferred significantly higher mean optimal spatial frequency and possessed broader spatial frequency tuning than the visually responsive neurons found in the SCi, the Sg and the CN. However, we could not find any significant difference between the mean optimal spatial frequency and spatial frequency bandwidth values in the SCi, the Sg and the CN.

6.1.2. Temporal frequency characteristics of different structures in the ascending tectofugal system

In connection with the temporal frequency properties of the neurons in the SCi, we found that the mean optimal temporal frequency and the temporal resolution of these cells were high, with a significant difference between the mean optimal temporal frequency and temporal resolution of the neurons in the SCs and the SCi. Thus, the neurons in the SCi preferred even higher temporal frequencies than those observed in the SCs. However, the mean optimal temporal frequency found in the SCi layers is comparable to those in the Sg, the CN, the AEV [92], the PMLS [90;101] and the AMLS [91], but higher than those in other visual cortical areas [93;98;102;103]. These results may suggest that the SCi is an important source of visual information in the high temporal frequency domain, relayed via the Sg of the posterior visual thalamus to the CN and to the cortical neurons in the LS areas and the AEV, structures, which take part in motion analysis [10;13;92;104;105].

The neurons in both the SCs and SCi layers are moderately tuned to temporal frequencies. We did not detect any significant difference between the temporal frequency tuning widths in the SCs and the SCi. The mean temporal tuning width of the collicular neurons is comparable to those in visual cortical areas A17 and A18 [96], the PMLS [90;101] and the LP-Pul of the thalamus [106], but lower than those in A19 [103], A21a [97;98], A21b [93] and higher than those in the AES cortex [92], the Sg and the CN.

When comparing the mean optimal temporal frequency and the temporal frequency bandwidth values of the neurons in the SCs, the SCi, the Sg and the CN, we could only

detect a statistically significant difference between the mean optimal temporal frequency in the SCs and the SCi layer neurons. In case of the temporal frequency tuning bandwidth, neurons in the SC differed significantly from those located in the Sg and the CN.

6.2. Multisensory response properties and multisensory integration in the basal ganglia

In the next set of our experiments our goal was to find new data concerning the multimodal representation of the environment in the basal ganglia of the mammalian brain. We recorded single-cell responses to visual, auditory, somatosensory and multisensory stimulation in the SNr and the CN, and found that multisensory stimulation elicited significantly different responses in the neurons than did the individual sensory components.

A majority of the recorded sensory neurons in the CN and the SNr were multisensory. A similarly high number of multisensory units (> 50%) were found in the SC, but the number of multisensory units described in the AEV (approximately 20%) is much lower [14;107-109].

Similarly to earlier findings in the CN, the majority of the investigated multisensory CN and SNr neurons displayed a significant multisensory cross-modal interaction [110]. Approximately three quarters of the interactions found in the SNr and the CN involved a cross-modal multisensory response enhancement, while the remaining quarter produced a multisensory response depression. Both facilitatory and inhibitory interactions were observed in each stimulus combinations. The magnitudes of the response enhancements and depressions varied widely among the CN and the SNr cells. The level was generally under 200%, although there were CN and SNr neurons that exhibited extremely strong multisensory effects, with enhancements up to 688% and 574%, respectively. The magnitudes of the multisensory indices calculated in the CN and the SNr were in the same range as those in the SC, but higher than those in the AES cortex [107;111]. Additionally, the investigated CN and SNr cells displayed different levels of the strength of the response. Similarly, as described earlier in the SC, both in the SNr and in the CN there was an inverse relationship between the response enhancement that the stimuli produced in combination and the effectiveness when they were presented alone [14]. Hence, the pairing of the least effective or ineffective unimodal stimuli induced a much larger multisensory

effect in the basal ganglia neurons than did the pairing of highly effective unimodal stimuli. This suggests that multisensory interactions in the basal ganglia improve the successful detection of environmental stimuli even when the unimodal sensory components presented alone have no significant meaning for the animal. Stanford et al. [84] have described a new classification of multisensory interactions in the feline SC. In contrast with the earlier commonly used facilitatory and inhibitory interactions, the multisensory effects were classified as subadditive, additive or superadditive. The interactions found in the CN and in the SNr that were either significantly facilitatory or significantly inhibitory in the classical approach of Meredith and Stein [14] were recalculated according to the new classification. All the facilitatory interactions in the basal ganglia proved to be either additive or superadditive, but never subadditive, while the inhibitory interactions were consistently subadditive.

In the SC, a multisensory response enhancement was often found when the visual and auditory stimuli originated from the same spatial position, while a multisensory response depression was mainly detected when the spatial disparity of the simultaneously presented auditory and visual stimuli was large [14;108;112]. In contrast with these findings in the SC, the neurons in the CN and the SNr often displayed a multisensory response depression to sensory stimuli originating from the same spatial position. In the SC, the strongest multisensory response enhancement was detected when the stimulus intensity used was not optimal, i.e. a weak auditory and/or visual stimulus [14]. In contrast with this, the CN and SNr neurons often revealed an extremely intensive multisensory enhancement when the optimal stimulus parameters were applied.

6.2.1. Modality distribution in the basal ganglia

The statistical analysis of the neuronal responses to separately presented visual or auditory or somatosensory stimulation suggested that a majority of the sensory units in the CN and the SNr were unimodal, in the sense that they responded to a statistically significant extent to only one of the individual sensory modalities tested. Similar results were found in the AES cortex and the SC, where a large majority of the units were likewise responsive to only one sensory modality in separate modality tests [14;82;113-115], the neuronal responses to multisensory stimulus complexes demonstrated that a significant

proportion of these units exhibited strong multisensory cross-modal interactions. We argue that any single neuron that exhibits a significant cross-modal response enhancement or depression must be classified as multisensory, despite responding to only one modality stimulation during the single modality tests [14]. Thus, analyses of the neuronal responsiveness to separate visual, auditory or somatosensory stimulation without any combination of the modalities may have strongly underrepresented the number of multisensory neurons in the basal ganglia [83;110;116;117].

The similar type of interactions revealed in the basal ganglia supports the notion concerning ascending multisensory tectofugal pathways to the CN and to the SNr [116]. The caudate body may receive its multisensory afferentation predominantly from the tectum and the AES cortex via the Sg nuclear complex of the thalamus [68;70;73;118]. The excitatory multisensory inputs of the SNr may originate from the CN [68;119] or from the tectum through direct [120] or indirect pathways [63;121-123] (Fig. 8). Accordingly, we assume that the CN and the SNr, as particular parts of a subcortical multisensory loop within the ascending tectofugal system, exert a critical function in multisensory integration. The multisensory integration in the CN and the SNr can presumably facilitate the processing of complex sensory stimuli as concerns the sensory feedback of motor actions controlled by the basal ganglia.

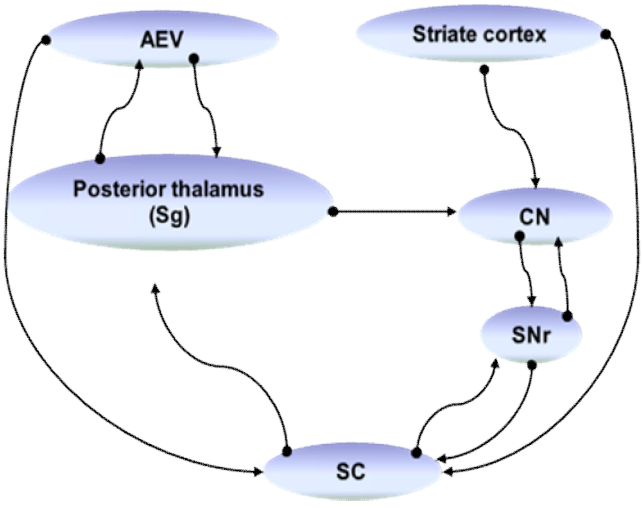

Figure 8. Subcortical multisensory loop in the ascending tectofugal system. Black arrows demonstrate the potential connections between the structures creating the tectal extrageniculate multisensory system. A loop is clearly seen between the SC, the posterior thalamus, the CN and the SNr.

7. Conclusions

Our results demonstrated that different structures (i.e. the SCs, the SCi, the Sg and the CN) in the ascending tectofugal system possess very similar spatio-temporal visual receptive field properties. Despite these similarities, we discerned significant differences in the mean optimal spatial and temporal frequencies and the spatial and temporal frequency tuning bandwidths between the pooled data on the SCs and the SCi layers, the Sg and the CN. The preference for low spatial frequencies combined with high temporal frequencies suggests that the neurons in both the SCs and the SCi, the Sg and the CN can detect large contours moving at high velocities well, but are unable to distinguish small details of the figures. These structures could possess a visuomotor function, such as organizing the complex, sensory-guided oculomotor and skeletomotor responses during the self-motion of the animal.

Moreover the CN and the SNr are capable of processing and integrating multisensory information. Multisensory information processing may result in a more accurate detection of the relevant sensory events in the complex multisensory environment. Accordingly, complex multisensory stimuli may possess effects or carry meanings that their individual components alone do not have. We suggest that the multisensory CN and SNr neurons may play a prominent role in sensorimotor integration and consequently allow the basal ganglia to participate in the adjustment of motor behavior in response to the environmental challenges.

Our results provide new information concerning the functioning of a subcortical multisensory loop, involving the SC, the CN and the SNr, within the ascending tectofugal system. Since a huge percent of multisensory information reaching the basal ganglia originates from the SC, we assume that these structures function together in the complex sensorimotor integration processes of the feline brain.

8. Summary

Electrophysiological recordings of single units in the SCi, the CN and the SNr were carried out extracellularly via tungsten microelectrodes in halothane-anesthetized, immobilized, artificially ventilated adult cats. Neuronal activities were recorded and correlated with the movement of the light stimulus and the auditory, the somatosensory, the bimodal and the trimodal stimuli by a computer and stored for further analysis as PSTHs. The net firing rate was calculated as the difference between the firing rates during the prestimulus and peristimulus intervals. The net firing rate was defined as a response when a t-test revealed a significant ($p<0.05$) difference between the two values.

In the first step of our analysis we compared the spatio-temporal frequency tuning properties of the SCs, the SCi, the Sg and the CN by one-way ANOVA analysis and Tukey post-hoc test. The summarized statistical analysis of the investigated structures revealed a significant difference among the optimal spatial frequencies of the investigated structures ($p<0.001$, $F_{(3,\ 374)}=16.376$). The post-hoc analysis showed that the mean optimal spatial frequency measured in the SCs was significantly higher than that of the SCi ($p<0.001$), the Sg ($p<0.001$) and the CN ($p<0.001$). In contrast to this, we found no significant difference ($p>0.05$) among the optimal spatial frequencies of the SCi, the Sg and the CN.

Similarly to the optimal spatial frequency values the summarized statistical analysis of the spatial frequency bandwidths revealed a significant difference among the investigated structures ($p<0.001$, $F_{(4,\ 236)}=6.317$). The post-hoc analysis showed that the spatial frequency bandwidth of the band-pass neurons in the SCs was significantly higher than that of the SCi ($p=0.004$), the Sg ($p<0.001$) and the CN ($p=0.006$). We found no significant difference ($p>0.05$) among the spatial frequency bandwidths of the SCi, the Sg and the CN.

The summarized statistical analysis of the investigated structures also revealed a significant difference among the optimal temporal frequencies of the investigated structures ($p=0.04$, $F_{(3,\ 314)}=2.807$). The post-hoc analysis showed that the mean optimal temporal frequency in the SCs was significantly lower than that of the SCi ($p=0.023$), the Sg ($p=0.012$) and the CN ($p=0.038$). In contrast we found no significant difference ($p>0.05$) among the optimal temporal frequencies of the SCi, the Sg and the CN.

Finally, similarly to the optimal temporal frequency, the summarized statistical analysis of the temporal frequency bandwidths revealed a significant difference among the investigated structures ($p<0.001$, $F_{(4, 307)}=13.797$). The post-hoc analysis showed that the temporal frequency tuning bandwidth of the neurons in the SCs and the SCi was not significantly different, but the temporal frequency bandwidths of both the SCs and the SCi neurons were significantly higher than that of the neurons in the Sg ($p<0.001$ in case of the SCs and $p<0.001$ in case of the SCi) and the CN ($p=0.023$ in case of the SCs and $p=0.03$ in case of the SCi). We found no significant difference ($p>0.05$) between the temporal frequency bandwidths of the Sg and the CN.

In the next set of our experiments our aim was to record the neuronal responses of the CN and SNr neurons to visual, auditory, somatosensory, bimodal and trimodal stimulations, thus, to reveal the multisensory information processing ability of the neurons in the basal ganglia. Afterwards we also investigated if these neurons were capable of integrating multisensory information deriving from different sources.

Altogether 302 single neurons in the CN and 480 single neurons in the SNr were recorded; 111 of these CN units and 124 of the nigral neurons exhibited excitatory responses to visual and/or auditory and/or somatosensory stimulation. The sensory properties of 77 CN and 75 SNr neurons were analyzed in detail.

We recorded unimodal as well as bimodal and trimodal neurons in both the CN and the SNr. A majority of the sensory neurons recorded in the CN and the SNr responded to visual or somatosensory stimulation. Only a relatively small proportion of the neurons displayed auditory sensitivity. The visual as well as the somatosensory and auditory receptive fields of the recorded neurons proved to be extremely large.

Fifty (65%) of the sensory CN neurons exhibited a unimodal character, reacting to only one investigated modality, while a smaller proportion (27, 35%) of them were multisensory, reacting to two or three different sensory modalities (7 visual-auditory, 9%; 9 visual-somatosensory, 12%; 3 auditory-somatosensory, 4% and 8 trimodal neurons, 10%). Similarly to the unimodal units, the sensory receptive fields of the multisensory CN neurons were extremely large, covering the whole of the approachable sensory field, i.e. a single trimodal CN neuron could process sensory information from the whole visual field

of the right eye, from the loudspeakers located throughout the whole 360° azimuth and from the whole body surface of the animal.

Thirty-eight (51%) of the 75 SNr units exhibited a unimodal character while the remaining 37 (49%) units were multisensory (5 visual-auditory, 7%; 16 visual-somatosensory, 21%; 5 auditory-somatosensory, 7%; 11 trimodal neurons, 14%). Similarly as for the unimodal SNr units, the receptive fields of the multisensory nigral neurons were extremely large.

We defined a neuron as multisensory either when it reacted to two or three different sensory modalities to a statistically significant extent, or when it reacted to only one sensory modality to a significant extent, but at least one of the ineffective modalities induced a multisensory cross–modal interaction. We found that 36 of the 77 investigated CN neurons (47%) and 41 of the 75 SNr neurons (55%) exhibited significant multisensory cross-modal interactions. Taking this definition into consideration we can say that the majority of the investigated sensory neurons in the CN and the SNr are actually multisensory.

We analyzed altogether 36 interactions between the CN units and 39 interactions between the SNr neurons. The large majority of the interactions in both structures were multisensory response enhancements and approximately one quarter of them were multisensory response depressions. We found significant facilitatory and inhibitory interactions in both structures in each multisensory stimulus combination tested.

According to our results we can suggest that the subcortical multisensory loop, involving the SC, the CN and the SNr, within the ascending tectofugal system of the feline brain provides the multisensory information processing background needed for the complex integrative sensorimotor functions exhibited mainly by the basal ganglia.

9. Acknowledgements

I respectfully thank Professor Dr. György Benedek and Dr. Attila Nagy who have served as my mentors and supervisors, and for the opportunity that I could work with them. I greatly appreciate their helpful and instructive guidance. I express my gratitude to Professor Dr. Gábor Jancsó for allowing me to participate in the Neuroscience Ph.D. Program. My special thanks go to Dr. Zsuzsanna Paróczy, Dr. Antal Berényi, Dr. Alice Rokszin, Dr. Ágnes Farkas, Gábor Braunitzer, Péter Gombkötő and Dr. Gabriella Eördegh for their help and friendship. I would like to acknowledge the help of Andrea Pető, Wioletta Waleszczyk and Marek Wypych, too.

I express my most sincere gratitude to Gabriella Dósai for her valuable technical assistance and for the preparation of high-quality figures for my thesis. Many thanks go to Péter Liszli for his expert help in solving hardware and software problems.

I would like to express my thanks to all of my colleagues and friends in the Department of Physiology for their support and kindness. It has been nice to work with them in this department.

My deepest thanks go to my parents, Dr. Sándor Márkus and Éva Csonták, my brother, Sándor Márkus, Dr. Imre Fejes and all of my relatives and friends for their continuous love and help in my life and scientific work.

Our experiments were supported by OTKA/Hungary grant F048396, OTKA/Hungary grant T042610, OTKA/Hungary grant 75156, OTKA/Hungary grant 68594 and ETT grant 429/2003.

10. Reference list

[1] B.E.Stein, T.R.Stanford, Multisensory integration: current issues from the perspective of the single neuron, Nat. Rev. Neurosci. 9 (2008) 255-266.

[2] G.E.Schneider, Two visual systems, Science 163 (1969) 895-902.

[3] R.H.Wurtz, J.E.Albano, Visual-motor function of the primate superior colliculus, Annu. Rev. Neurosci. 3 (1980) 189-226.

[4] P.H.Schiller, E.J.Tehovnik, Look and see: how the brain moves your eyes about, Prog. Brain Res. 134 (2001) 127-142.

[5] R.W.Rodieck, M.Watanabe, Survey of the morphology of macaque retinal ganglion cells that project to the pretectum, superior colliculus, and parvicellular laminae of the lateral geniculate nucleus, J. Comp Neurol. 338 (1993) 289-303.

[6] P.H.Schiller, J.G.Malpeli, Properties and tectal projections of monkey retinal ganglion cells, J Neurophysiol. 40 (1977) 428-445.

[7] J.K.Harting, B.V.Updyke, D.P.Van Lieshout, Corticotectal projections in the cat: anterograde transport studies of twenty-five cortical areas, J. Comp Neurol. 324 (1992) 379-414.

[8] M.E.Wilson, M.J.Toyne, Retino-tectal and cortico-tectal projections in Macaca mulatta, Brain Res. 24 (1970) 395-406.

[9] J.Graham, Some topographical connections of the striate cortex with subcortical structures in Macaca fascicularis, Exp. Brain Res. 47 (1982) 1-14.

[10] B.P.Abramson, L.M.Chalupa, Multiple pathways from the superior colliculus to the extrageniculate visual thalamus of the cat, J. Comp Neurol. 271 (1988) 397-418.

[11] P.J.May, The mammalian superior colliculus: laminar structure and connections, Prog. Brain Res. 151 (2006) 321-378.

[12] Y.Y.Katoh, G.Benedek, Organization of the colliculo-suprageniculate pathway in the cat: a wheat germ agglutinin-horseradish peroxidase study, J. Comp Neurol. 352 (1995) 381-397.

[13] Y.Y.Katoh, G.Benedek, S.Deura, Bilateral projections from the superior colliculus to the suprageniculate nucleus in the cat: a WGA-HRP/double fluorescent tracing study, Brain Res. 669 (1995) 298-302.

[14] M.A.Meredith, B.E.Stein, Visual, auditory, and somatosensory convergence on cells in superior colliculus results in multisensory integration, J. Neurophysiol. 56 (1986) 640-662.

[15] J.M.Sprague, The superior colliculus and pretectum in visual behavior, Invest Ophthalmol. 11 (1972) 473-482.

[16] J.M.Sprague, The role of the superior colliculus in facilitating visual attention and form perception, Proc. Natl. Acad. Sci. U. S. A 88 (1991) 1286-1290.

[17] R.J.Cowie, D.L.Robinson, Subcortical contributions to head movements in macaques. I. Contrasting effects of electrical stimulation of a medial pontomedullary region and the superior colliculus, J Neurophysiol. 72 (1994) 2648-2664.

[18] E.G.Freedman, D.L.Sparks, Activity of cells in the deeper layers of the superior colliculus of the rhesus monkey: evidence for a gaze displacement command, J Neurophysiol. 78 (1997) 1669-1690.

[19] W.Werner, Neurons in the primate superior colliculus are active before and during arm movements to visual targets, Eur. J Neurosci. 5 (1993) 335-340.

[20] A.Nagy, W.Kruse, S.Rottmann, S.Dannenberg, K.P.Hoffmann, Somatosensory-motor neuronal activity in the superior colliculus of the primate, Neuron 52 (2006) 525-534.

[21] M.T.Wallace, M.A.Meredith, B.E.Stein, Converging influences from visual, auditory, and somatosensory cortices onto output neurons of the superior colliculus, J. Neurophysiol. 69 (1993) 1797-1809.

[22] H.R.Clemo, B.E.Stein, Somatosensory cortex: a 'new' somatotopic representation, Brain Res. 235 (1982) 162-168.

[23] L.Mucke, M.Norita, G.Benedek, O.Creutzfeldt, Physiologic and anatomic investigation of a visual cortical area situated in the ventral bank of the anterior ectosylvian sulcus of the cat, Exp. Brain Res. 46 (1982) 1-11.

[24] C.R.Olson, A.M.Graybiel, An outlying visual area in the cerebral cortex of the cat, Prog. Brain Res. 58 (1983) 239-245.

[25] J.C.Clarey, D.R.Irvine, Auditory response properties of neurons in the anterior ectosylvian sulcus of the cat, Brain Res. 386 (1986) 12-19.

[26] D.M.Berson, Cat lateral suprasylvian cortex: Y-cell inputs and corticotectal projection, J. Neurophysiol. 53 (1985) 544-556.

[27] L.K.Wilkinson, M.A.Meredith, B.E.Stein, The role of anterior ectosylvian cortex in cross-modality orientation and approach behavior, Exp. Brain Res. 112 (1996) 1-10.

[28] W.Jiang, H.Jiang, B.E.Stein, Two corticotectal areas facilitate multisensory orientation behavior, J. Cogn Neurosci. 14 (2002) 1240-1255.

[29] W.Jiang, H.Jiang, B.E.Stein, Neonatal cortical ablation disrupts multisensory development in superior colliculus, J. Neurophysiol. 95 (2006) 1380-1396.

[30] M.T.Wallace, B.E.Stein, Cross-modal synthesis in the midbrain depends on input from cortex, J. Neurophysiol. 71 (1994) 429-432.

[31] J.C.Alvarado, J.W.Vaughan, T.R.Stanford, B.E.Stein, Multisensory versus unisensory integration: contrasting modes in the superior colliculus, J. Neurophysiol. 97 (2007) 3193-3205.

[32] W.Jiang, M.T.Wallace, H.Jiang, J.W.Vaughan, B.E.Stein, Two cortical areas mediate multisensory integration in superior colliculus neurons, J. Neurophysiol. 85 (2001) 506-522.

[33] B.E.Stein, R.F.Spencer, S.B.Edwards, Corticotectal and corticothalamic efferent projections of SIV somatosensory cortex in cat, J. Neurophysiol. 50 (1983) 896-909.

[34] B.Stricanne, R.A.Andersen, P.Mazzoni, Eye-centered, head-centered, and intermediate coding of remembered sound locations in area LIP, J Neurophysiol. 76 (1996) 2071-2076.

[35] A.P.Batista, C.A.Buneo, L.H.Snyder, R.A.Andersen, Reach plans in eye-centered coordinates, Science 285 (1999) 257-260.

[36] Y.E.Cohen, R.A.Andersen, A common reference frame for movement plans in the posterior parietal cortex, Nat. Rev. Neurosci. 3 (2002) 553-562.

[37] M.Avillac, S.Deneve, E.Olivier, A.Pouget, J.R.Duhamel, Reference frames for representing visual and tactile locations in parietal cortex, Nat. Neurosci. 8 (2005) 941-949.

[38] T.Sugihara, M.D.Diltz, B.B.Averbeck, L.M.Romanski, Integration of auditory and visual communication information in the primate ventrolateral prefrontal cortex, J. Neurosci. 26 (2006) 11138-11147.

[39] L.M.Romanski, Representation and integration of auditory and visual stimuli in the primate ventral lateral prefrontal cortex, Cereb. Cortex 17 Suppl 1 (2007) i61-i69.

[40] N.E.Barraclough, D.Xiao, C.I.Baker, M.W.Oram, D.I.Perrett, Integration of visual and auditory information by superior temporal sulcus neurons responsive to the sight of actions, J Cogn Neurosci. 17 (2005) 377-391.

[41] G.A.Calvert, R.Campbell, M.J.Brammer, Evidence from functional magnetic resonance imaging of crossmodal binding in the human heteromodal cortex, Curr. Biol. 10 (2000) 649-657.

[42] A.A.Ghazanfar, C.Chandrasekaran, N.K.Logothetis, Interactions between the superior temporal sulcus and auditory cortex mediate dynamic face/voice integration in rhesus monkeys, J. Neurosci. 28 (2008) 4457-4469.

[43] G.A.Calvert, P.C.Hansen, S.D.Iversen, M.J.Brammer, Detection of audio-visual integration sites in humans by application of electrophysiological criteria to the BOLD effect, Neuroimage. 14 (2001) 427-438.

[44] J.Driver, T.Noesselt, Multisensory interplay reveals crossmodal influences on 'sensory-specific' brain regions, neural responses, and judgments, Neuron 57 (2008) 11-23.

[45] J.K.Bizley, F.R.Nodal, V.M.Bajo, I.Nelken, A.J.King, Physiological and anatomical evidence for multisensory interactions in auditory cortex, Cereb. Cortex 17 (2007) 2172-2189.

[46] C.Cappe, P.Barone, Heteromodal connections supporting multisensory integration at low levels of cortical processing in the monkey, Eur. J Neurosci. 22 (2005) 2886-2902.

[47] K.S.Rockland, H.Ojima, Multisensory convergence in calcarine visual areas in macaque monkey, Int. J Psychophysiol. 50 (2003) 19-26.

[48] A.Falchier, S.Clavagnier, P.Barone, H.Kennedy, Anatomical evidence of multimodal integration in primate striate cortex, J Neurosci. 22 (2002) 5749-5759.

[49] M.A.Meredith, L.R.Keniston, L.R.Dehner, H.R.Clemo, Crossmodal projections from somatosensory area SIV to the auditory field of the anterior ectosylvian sulcus (FAES) in Cat: further evidence for subthreshold forms of multisensory processing, Exp. Brain Res. 172 (2006) 472-484.

[50] W.J.Waleszczyk, C.Wang, W.Burke, B.Dreher, Velocity response profiles of collicular neurons: parallel and convergent visual information channels, Neuroscience 93 (1999) 1063-1076.

[51] K.Dec, W.J.Waleszczyk, A.Wrobel, B.A.Harutiunian-Kozak, The spatial substructure of visual receptive fields in the cat's superior colliculus, Arch. Ital. Biol. 139 (2001) 337-356.

[52] M.Hashemi-Nezhad, C.Wang, W.Burke, B.Dreher, Area 21a of cat visual cortex strongly modulates neuronal activities in the superior colliculus, J. Physiol 550 (2003) 535-552.

[53] B.Dreher, K.P.Hoffmann, Properties of excitatory and inhibitory regions in the receptive fields of single units in the cat's superior colliculus, Exp. Brain Res. 16 (1973) 333-353.

[54] K.Ogasawara, J.G.McHaffie, B.E.Stein, Two visual corticotectal systems in cat, J. Neurophysiol. 52 (1984) 1226-1245.

[55] J.D.Mendola, B.R.Payne, Direction selectivity and physiological compensation in the superior colliculus following removal of areas 17 and 18, Vis. Neurosci. 10 (1993) 1019-1026.

[56] R.B.Pinter, L.R.Harris, Temporal and spatial response characteristics of the cat superior colliculus, Brain Res. 207 (1981) 73-94.

[57] K.K.De Valois, R.L.De Valois, E.W.Yund, Responses of striate cortex cells to grating and checkerboard patterns, J Physiol 291 (1979) 483-505.

[58] S.Guirado, M.A.Real, J.C.Davila, The ascending tectofugal visual system in amniotes: new insights, Brain Res. Bull. 66 (2005) 290-296.

[59] M.Takada, H.Tokuno, Y.Ikai, N.Mizuno, Direct projections from the entopeduncular nucleus to the lower brainstem in the rat, J Comp Neurol. 342 (1994) 409-429.

[60] J.M.Deniau, G.Chevalier, The lamellar organization of the rat substantia nigra pars reticulata: distribution of projection neurons, Neuroscience 46 (1992) 361-377.

[61] P.Redgrave, L.Marrow, P.Dean, Topographical organization of the nigrotectal projection in rat: evidence for segregated channels, Neuroscience 50 (1992) 571-595.

[62] K.Takakusaki, K.Saitoh, H.Harada, M.Kashiwayanagi, Role of basal ganglia-brainstem pathways in the control of motor behaviors, Neurosci. Res. 50 (2004) 137-151.

[63] H.Jiang, B.E.Stein, J.G.McHaffie, Opposing basal ganglia processes shape midbrain visuomotor activity bilaterally, Nature 423 (2003) 982-986.

[64] O.Hikosaka, Y.Takikawa, R.Kawagoe, Role of the basal ganglia in the control of purposive saccadic eye movements, Physiol Rev. 80 (2000) 953-978.

[65] Y.D.Van der Werf, M.P.Witter, H.J.Groenewegen, The intralaminar and midline nuclei of the thalamus. Anatomical and functional evidence for participation in processes of arousal and awareness, Brain Res. Brain Res. Rev. 39 (2002) 107-140.

[66] M.Takada, K.Itoh, Y.Yasui, T.Sugimoto, N.Mizuno, Topographical projections from the posterior thalamic regions to the striatum in the cat, with reference to possible tecto-thalamo-striatal connections, Exp. Brain Res. 60 (1985) 385-396.

[67] J.Feger, M.Bevan, A.R.Crossman, The projections from the parafascicular thalamic nucleus to the subthalamic nucleus and the striatum arise from separate neuronal populations: a comparison with the corticostriatal and corticosubthalamic efferents in a retrograde fluorescent double-labelling study, Neuroscience 60 (1994) 125-132.

[68] J.G.McHaffie, T.R.Stanford, B.E.Stein, V.Coizet, P.Redgrave, Subcortical loops through the basal ganglia, Trends Neurosci. 28 (2005) 401-407.

[69] D.M.Berson, A.M.Graybiel, Tectorecipient zone of cat lateral posterior nucleus: evidence that collicular afferents contain acetylcholinesterase, Exp. Brain Res. 84 (1991) 478-486.

[70] J.K.Harting, B.V.Updyke, D.P.Van Lieshout, The visual-oculomotor striatum of the cat: functional relationship to the superior colliculus, Exp. Brain Res. 136 (2001) 138-142.

[71] B.V.Updyke, Projections from visual areas of the middle suprasylvian sulcus onto the lateral posterior complex and adjacent thalamic nuclei in cat, J Comp Neurol. 201 (1981) 477-506.

[72] D.Raczkowski, A.C.Rosenquist, Connections of the multiple visual cortical areas with the lateral posterior-pulvinar complex and adjacent thalamic nuclei in the cat, J Neurosci. 3 (1983) 1912-1942.

[73] J.K.Harting, B.V.Updyke, D.P.Van Lieshout, Striatal projections from the cat visual thalamus, Eur. J. Neurosci. 14 (2001) 893-896.

[74] O.Hikosaka, R.H.Wurtz, Visual and oculomotor functions of monkey substantia nigra pars reticulata. III. Memory-contingent visual and saccade responses, J Neurophysiol. 49 (1983) 1268-1284.

[75] K.E.Krout, A.D.Loewy, G.W.Westby, P.Redgrave, Superior colliculus projections to midline and intralaminar thalamic nuclei of the rat, J Comp Neurol. 431 (2001) 198-216.

[76] G.Chevalier, J.M.Deniau, Spatio-temporal organization of a branched tecto-spinal/tecto-diencephalic neuronal system, Neuroscience 12 (1984) 427-439.

[77] A.Nagy, G.Eordegh, M.Norita, G.Benedek, Visual receptive field properties of neurons in the caudate nucleus, Eur. J. Neurosci. 18 (2003) 449-452.

[78] E.Mengual, H.S.de las, E.Erro, J.L.Lanciego, J.M.Gimenez-Amaya, Thalamic interaction between the input and the output systems of the basal ganglia, J Chem. Neuroanat. 16 (1999) 187-200.

[79] M.Y.Villeneuve, C.Casanova, On the use of isoflurane versus halothane in the study of visual response properties of single cells in the primary visual cortex, J. Neurosci. Methods 129 (2003) 19-31.

[80] J.D.Pettigrew, M.L.Cooper, G.G.Blasdel, Improved use of tapetal reflection for eye-position monitoring, Invest Ophthalmol. Vis. Sci. 18 (1979) 490-495.

[81] P.O.Bishop, W.Kozak, G.J.Vakkur, Some quantitative aspects of the cat's eye: axis and plane of reference, visual field co-ordinates and optics, J Physiol 163 (1962) 466-502.

[82] M.A.Meredith, B.E.Stein, Interactions among converging sensory inputs in the superior colliculus, Science 221 (1983) 389-391.

[83] G.Pouderoux, E.Freton, Patterns of unit responses to visual stimuli in the cat caudate nucleus under chloralose anesthesia, Neurosci. Lett. 11 (1979) 53-58.

[84] T.R.Stanford, S.Quessy, B.E.Stein, Evaluating the operations underlying multisensory integration in the cat superior colliculus, J. Neurosci. 25 (2005) 6499-6508.

[85] W.J.Waleszczyk, A.Nagy, M.Wypych, A.Berenyi, Z.Paroczy, G.Eordegh, A.Ghazaryan, G.Benedek, Spectral receptive field properties of neurons in the feline superior colliculus, Exp. Brain Res. 181 (2007) 87-98.

[86] R.Sireteanu, K.P.Hoffmann, Relative frequency and visual resolution of X- and Y-cells in the LGN of normal and monocularly deprived cats: interlaminar differences, Exp. Brain Res. 34 (1979) 591-603.

[87] M.Sur, S.M.Sherman, Linear and nonlinear W-cells in C-laminae of the cat's lateral geniculate nucleus, J Neurophysiol. 47 (1982) 869-884.

[88] A.B.Saul, A.L.Humphrey, Spatial and temporal response properties of lagged and nonlagged cells in cat lateral geniculate nucleus, J Neurophysiol. 64 (1990) 206-224.

[89] M.Di Stefano, M.C.Morrone, D.C.Burr, Visual acuity of neurones in the cat lateral suprasylvian cortex, Brain Res. 331 (1985) 382-385.

[90] T.J.Zumbroich, C.Blakemore, Spatial and temporal selectivity in the suprasylvian visual cortex of the cat, J Neurosci. 7 (1987) 482-500.

[91] B.G.Ouellette, K.Minville, J.Faubert, C.Casanova, Simple and complex visual motion response properties in the anterior medial bank of the lateral suprasylvian cortex, Neuroscience 123 (2004) 231-245.

[92] A.Nagy, G.Eordegh, G.Benedek, Spatial and temporal visual properties of single neurons in the feline anterior ectosylvian visual area, Exp. Brain Res. 151 (2003) 108-114.

[93] E.Tardif, F.Lepore, J.P.Guillemot, Spatial properties and direction selectivity of single neurons in area 21b of the cat, Neuroscience 97 (2000) 625-634.

[94] L.Maffei, A.Fiorentini, The visual cortex as a spatial frequency analyser, Vision Res. 13 (1973) 1255-1267.

[95] H.M.Eggers, C.Blakemore, Physiological basis of anisometropic amblyopia, Science 201 (1978) 264-267.

[96] J.A.Movshon, I.D.Thompson, D.J.Tolhurst, Spatial and temporal contrast sensitivity of neurones in areas 17 and 18 of the cat's visual cortex, J Physiol 283 (1978) 101-120.

[97] E.Tardif, A.Bergeron, F.Lepore, J.P.Guillemot, Spatial and temporal frequency tuning and contrast sensitivity of single neurons in area 21a of the cat, Brain Res. 716 (1996) 219-223.

[98] J.W.Morley, R.M.Vickery, Spatial and temporal frequency selectivity of cells in area 21a of the cat, J Physiol 501 (Pt 2) (1997) 405-413.

[99] E.Tardif, L.Richer, A.Bergeron, F.Lepore, J.P.Guillemot, Spatial resolution and contrast sensitivity of single neurons in area 19 of split-chiasm cats: a comparison with primary visual cortex, Eur. J Neurosci. 9 (1997) 1929-1939.

[100] K.Minville, C.Casanova, Spatial frequency processing in posteromedial lateral suprasylvian cortex does not depend on the projections from the striate-recipient zone of the cat's lateral posterior-pulvinar complex, Neuroscience 84 (1998) 699-711.

[101] M.C.Morrone, M.Di Stefano, D.C.Burr, Spatial and temporal properties of neurons of the lateral suprasylvian cortex of the cat, J Neurophysiol. 56 (1986) 969-986.

[102] C.Casanova, Response properties of neurons in area 17 projecting to the striate-recipient zone of the cat's lateralis posterior-pulvinar complex: comparison with cortico-tectal cells, Exp. Brain Res. 96 (1993) 247-259.

[103] A.Bergeron, E.Tardif, F.Lepore, J.P.Guillemot, Spatial and temporal matching of receptive field properties of binocular cells in area 19 of the cat, Neuroscience 86 (1998) 121-134.

[104] T.P.Hicks, C.A.Stark, W.A.Fletcher, Origins of afferents to visual suprageniculate nucleus of the cat, J. Comp Neurol. 246 (1986) 544-554.

[105] C.R.Olson, A.M.Graybiel, Ectosylvian visual area of the cat: location, retinotopic organization, and connections, J Comp Neurol. 261 (1987) 277-294.

[106] C.Casanova, R.D.Freeman, J.P.Nordmann, Monocular and binocular response properties of cells in the striate-recipient zone of the cat's lateral posterior-pulvinar complex, J Neurophysiol. 62 (1989) 544-557.

[107] M.T.Wallace, M.A.Meredith, B.E.Stein, Integration of multiple sensory modalities in cat cortex, Exp. Brain Res. 91 (1992) 484-488.

[108] M.T.Wallace, B.E.Stein, Sensory organization of the superior colliculus in cat and monkey, Prog. Brain Res. 112 (1996) 301-311.

[109] B.E.Stein, Neural mechanisms for synthesizing sensory information and producing adaptive behaviors, Exp. Brain Res. 123 (1998) 124-135.

[110] E.H.Chudler, K.Sugiyama, W.K.Dong, Multisensory convergence and integration in the neostriatum and globus pallidus of the rat, Brain Res. 674 (1995) 33-45.

[111] M.A.Meredith, J.W.Nemitz, B.E.Stein, Determinants of multisensory integration in superior colliculus neurons. I. Temporal factors, J. Neurosci. 7 (1987) 3215-3229.

[112] M.A.Meredith, B.E.Stein, Spatial determinants of multisensory integration in cat superior colliculus neurons, J. Neurophysiol. 75 (1996) 1843-1857.

[113] G.Benedek, L.Mucke, M.Norita, B.Albowitz, O.D.Creutzfeldt, Anterior ectosylvian visual area (AEV) of the cat: physiological properties, Prog. Brain Res. 75 (1988) 245-255.

[114] G.Benedek, G.Eordegh, Z.Chadaide, A.Nagy, Distributed population coding of multisensory spatial information in the associative cortex, Eur. J. Neurosci. 20 (2004) 525-529.

[115] T.P.Hicks, G.Benedek, G.A.Thurlow, Modality specificity of neuronal responses within the cat's insula, J. Neurophysiol. 60 (1988) 422-437.

[116] A.Nagy, Z.Paroczy, M.Norita, G.Benedek, Multisensory responses and receptive field properties of neurons in the substantia nigra and in the caudate nucleus, Eur. J. Neurosci. 22 (2005) 419-424.

[117] C.Magarinos-Ascone, E.Garcia-Austt, W.Buno, Polymodal sensory and motor convergence in substantia nigra neurons of the awake monkey, Brain Res. 646 (1994) 299-302.

[118] M.Norita, J.G.McHaffie, H.Shimizu, B.E.Stein, The corticostriatal and corticotectal projections of the feline lateral suprasylvian cortex demonstrated with anterograde biocytin and retrograde fluorescent techniques, Neurosci. Res. 10 (1991) 149-155.

[119] M.Rodriguez, P.Abdala, J.A.Obeso, Excitatory responses in the 'direct' striatonigral pathway: effect of nigrostriatal lesion, Mov Disord. 15 (2000) 795-803.

[120] E.Comoli, V.Coizet, J.Boyes, J.P.Bolam, N.S.Canteras, R.H.Quirk, P.G.Overton, P.Redgrave, A direct projection from superior colliculus to substantia nigra for detecting salient visual events, Nat. Neurosci. 6 (2003) 974-980.

[121] H.Kita, S.T.Kitai, Efferent projections of the subthalamic nucleus in the rat: light and electron microscopic analysis with the PHA-L method, J Comp Neurol. 260 (1987) 435-452.

[122] H.Tokuno, M.Takada, Y.Ikai, N.Mizuno, Direct projections from the deep layers of the superior colliculus to the subthalamic nucleus in the rat, Brain Res. 639 (1994) 156-160.

[123] S.J.Lokwan, P.G.Overton, M.S.Berry, D.Clark, Stimulation of the pedunculopontine tegmental nucleus in the rat produces burst firing in A9 dopaminergic neurons, Neuroscience 92 (1999) 245-254.